

A Therapeutic Device for Surgical Robots

Veronika Ivanova

Institute of Robotics

Bulgarian Academy of Science

Acad. Georgi Bonchev Str., block 1

1113 Sofia, Bulgaria

ivanowa.w@abv.bg

Abstract: The medical area is evolving toward greater application of non-invasive and minimally invasive therapy. Minimally-invasive surgery is very popular medical intervention for diagnoses and treatment of some human diseases. In recent decades the applying of these procedures in surgical rooms is increasing and it leads to development of innovative techniques, tools and methods for their execution. A number of problems related to minimally-invasive surgery are solved by introduction of robots in surgical area. In this article our effort to design a therapeutic device for surgical robots is described. In contrast to other research and development in the field of local tumor therapy, the paper discusses a device for surgical robots that simultaneously examines biomechanical tissue characteristics and then applies local tumor therapy. Ultimate aim of the work is a design of a compact, convenient, simplified, better possibilities and suitable price devices thereby and the small hospitals to have access to these systems and patient benefit from it. This paper is a continuation of previous work in the surgical robotics area.

Keywords: *Therapeutics device, local radiations source, tumor, minimally-invasive surgery, surgical robots, High-Intensity Focused Ultrasound*

1. Introduction

Major gallbladder diseases are stones and carcinoma. Tumors are rare diseases of the biliary tract. Correctly gallbladder function is essential to the digestive

process. When gallbladder cancer is caught early, removing a gallbladder or part of the bile duct may eliminate all the cancerous cells. Gallbladder cancer does not have any proven prevention methods. The causes of the disease, such as gallstones, cannot be prevented from forming in the gallbladder. Two main types of gallbladder cancer tumors are typical-adenocarcinoma and non-adenocarcinoma. There is a lot of methods for diagnostics of gallbladder carcinoma: Blood tests, Ultrasound Computerized tomography (CT) scan Magnetic resonance imaging (MRI) Endoscopic retrograde cholangio pancreatography (ERCP) Biopsy, Laparoscopy, and etc. Tumors tend to be harder than the surrounding tissue, and not possible indicate their presence, size and exact location without tactile sense when diagnostics is performed by laparoscopic procedure. Many gallbladder cancers are discovered after a laboratory examination of a gallbladder that's been removed for other reasons.

The main method for the treatment of tumors is their surgical removal. However, some of them are resectable when discovered. Therefore, novel approaches to the tumor treatment must be sought and tested. Various tissue ablation methods are used in surgery such as radio frequency currents, microwaves, laser, heat conduction sources and ultrasound. Ultrasound has some advantages, such as the possibility of deeper tissue treatment, improved focusing on target tissue through its small wavelengths and precise shape control and place of energy deposition [1, 2] Recent years focused on high intensity ultrasound (HIFU) and magnetic resonance focused ultrasound (MRgFUS) have proven effective as non-invasive soft tissue ablation methods. The methods are applied for treatment thousands of patients worldwide [3, 4, 5], with MRgFUS being offered as an alternative to broad set of surgical procedures. High Intensity Focused Ultrasound (HIFU) offers a new approach in the treatment of cancer. HIFU is an effective non-invasive technique for cancer treatment particularly for high surgical-risk patients The many advantages of HIFU justify the increasing interest in the clinical applications of this approach: Reduced toxicity compared to other techniques; non-invasive method and minimal pain; relatively inexpensive procedure and technique; suitable for patients with high surgical risk; leaves no scars on the patient; short risk of infection; recovery is faster compared to traditional surgical techniques; bleeding during the procedure can be stopped with ultrasound; precise delivery of energy to a target point without disturbing the integrity of the skin; system maintenance costs are low; minor side effects on the surrounding tissue [6], patient safety with minimal side effect, the technique is precise and easy to apply.

The beam is focused on a small part of the tissue and is produced quickly and intensively heating. High tissue temperatures (up to 100°C) can lead to localized tissue ablation. HIFU-induced lesions can occur at any depth in the

organ by directing the acoustic focus to the desired location. The intermediate tissue remains intact because it is outside the acoustic focus [7].

The heat in HIFU causes a rapid rise temperature in the tissue to more than 60 °C, resulting in immediate cellular death in most tissues when lasting more than 1 s [8]. An ultrasound beam causes high intensity at the focal point in a small volume of about 1 mm in diameter and about 10 mm in length [9], which minimizes potential tissue damage outside the focal area. Thermal damage to tissues due to exposure to high temperature depends almost linearly on length from the exposure time and exponentially with increasing temperature [9].

HIFU devices consist of two major components- a piezoelectric ultrasound transducer to deliver the therapeutic ultrasound beam and an imaging modality used for guidance. They are the most common a concave focusing transducer with fixed aperture and focal length (Fig. 1a), a phased array transducer comprising multiple transducers located on the truncated surface of a spherical surface (Fig. 1b), or a planar transducer/fully filled phased array (Fig. 1c) are used.

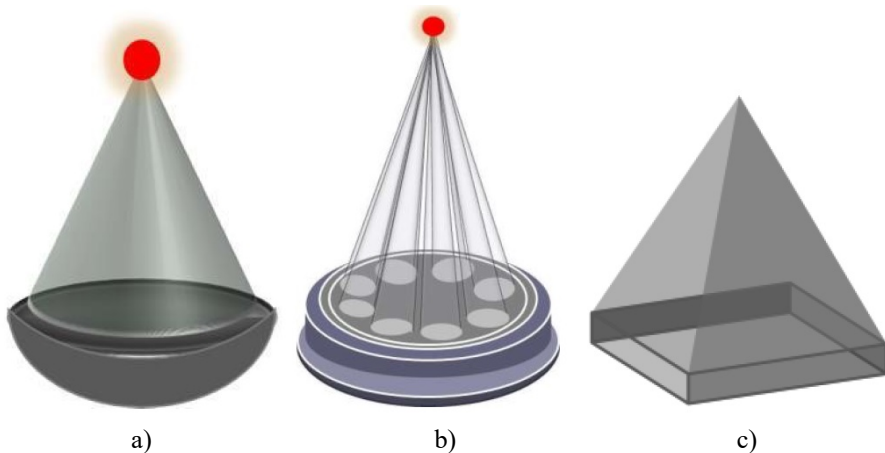


Fig. 1. Schematic of a focusing transducer.

Mechanical movement of the transducer determines the position of the focal spot, with electronic control of the ultrasound beam allowing fine control of the location of the focal spot. The imaging modality used for guidance is the second HIFU component. For effective treatment, real-time imaging during the therapeutic procedure is essential. Imaging methods that have been used to monitor treatment are sonography and magnetic resonance imaging (MRI).

A number of experimental studies have been done with HIFU to prove its effectiveness in treating tumors. Clinical studies using High-intensity focused ultrasound (HIFU) for tumor treatment to rats indicate that of tumor growth is significant inhibition. Significantly improved survival rates are noted in HIFU-

treated animals. This research resultant assume that HIFU may be a useful therapy for local treatment of some type of tumors [10] and it is an attractive non-invasive alternative method for small in size tumors. This experiments support the concept that HIFU can indeed kill tumor cells, presumably by the development of intense lethal heat production within the tumor and due to the tumor's blood supply being cut off. Experimental studies have been applied to significantly larger animals such as rabbits, with treatment taking significantly less time, as well as superficial lesions and tumors at different depths in the organ. With successful application of this method of resection (surgical intervention) can be avoided.

HIFU clinical studies relegated to kidney tumor treatment have reported for promising results [11,12, 13,14, 15]. Liver cancer is one of the most common and often one of the most difficult to treat. Some research includes HIFU tumor therapy device and overall, HIFU has been clinically demonstrated to prolong survival period in liver cancer patients [16, 17, 18 19, 20]. HIFU has been used effectively to treat various types of breast cancer, with some studies using custom-made HIFU systems at frequencies from 1.5 to 1.7 MHz [21,22] Results have been associated with tumor destruction and loss of proliferation [23]. Some studies have shown a disease-free survival rate of 95%, a recurrence-free survival rate of 89%, and a 90% reduction in tumor size in treated patients [24].

During therapeutic treatment the HIFU devices have to be together applied with diagnostic systems to provide safety, better navigation, and assessment of vascularity. The advantage of HIFU that it can induce rapid cell death by coagulation necrosis of selected tissue areas made it a candidate for direct and rapid treatment of tumors and to achieve hemostasis, as shown in animal experiments [25, 26, 27, 28]. Experimental results show that there is a relationship between the optimum frequency and target depth determined by the average attenuation coefficient of the medium for HIFU applications [29].

Since the start of cancer treatment, many technological advances and new treatment strategies have been implemented to optimize treatment delivery and to decrease the occurrence of side effects in healthy tissues [30].

With the introduction of robots into people's daily lives, their lives are made easier. Modern trends in this directions are well described in a number of publications [31, 32, 33, 34]. From the industry, these machines also move into the surgical theaters. Many people fear that robots or full automation may someday take their jobs, but this is simply not the case. Robots bring more advantages than disadvantages. A number of problems are solved with the help of robotics in the operating room. Advances in robotics and mechatronics can be used to optimize cancer treatment. Intelligent medical technologies, robotic and mechatronics systems over the past decades have given oncologists the capability to personalize treatments for accurate delivery of therapeutic dose based on

clinical parameters and anatomical information. Two schemes working simultaneously, will enable further widening of the possibilities of cancer therapy: technological improvement for better patient treatment, including advanced image guidance and particle therapy, and novel methods for treatment of patients with biomarker-guided prescription, combined treatment modalities and adaptation of treatment during its course. Very important for oncology is Radiation Therapy. Most medical treatment schemes including radiation therapy.

This paper discusses our effort for design of a device to surgical robots that simultaneously examines biomechanical tissue characteristics and then applies local tumor therapy.

The work is organized as follow: Section 2 includes an instrument for therapy in laparoscopic surgery. Section 3 reports mode for studying the biomechanical properties of tissues. Section 4 describes therapeutics mode. In section 5 are shown some experimental results. Finally, section 6 concludes the paper and points at the intentions for future work.

2. An Instrument for therapy in laparoscopic surgery

An instrument for a therapy (see Fig.1) is a device that incorporates a linear step motor, positioning and force sensors, a FR emitter and mechanical structure. The module for therapy is designed for programmable irradiation of FEM (2.44 GHz – 2.508 GHz). The radiation is local, within a radius of 1 mm from the emitter. It is possible change of the intensity and frequency of the SDR radiation as a function of the time. The broadcast signal poses four intensities. The radio signal acts on the emitters in direct contact with the emitter, the signal attenuation being realized at 100% off the sphere, with a radius of 1 mm and the center of the tool. A model of therapeutic device for surgical robots is shown in Fig. 2.



Fig. 2. A model of therapeutic device for surgical robots.

The instrument includes the following structure:

- 1) Two high-precision channels for sensors;
- 2) Fast and precise analogue to digital converter to measure force;
- 3) Local indication for direct control of the applied force on the sensor;
- 4) Different channels for transferring measured data to the control system of the device;
- 5) Radio wave channel for transmitting of radio signals.

The instrument can work in two modes: The first one studying the biomechanical properties of tissues includes smart transmitting and calculating work.

1) Transparent SubMode (smart transmitter) – directly transfers measured data to the next control system. In this case the calculation of the P control is done in the control system of the device;

2) Calculating SubMode – the P control is built in the program inside the control module. In this case the control module generates a direct task for implementation.

A block diagram of the developed communication concept for a device digital controller component in the first mode is shown in Fig. 3.

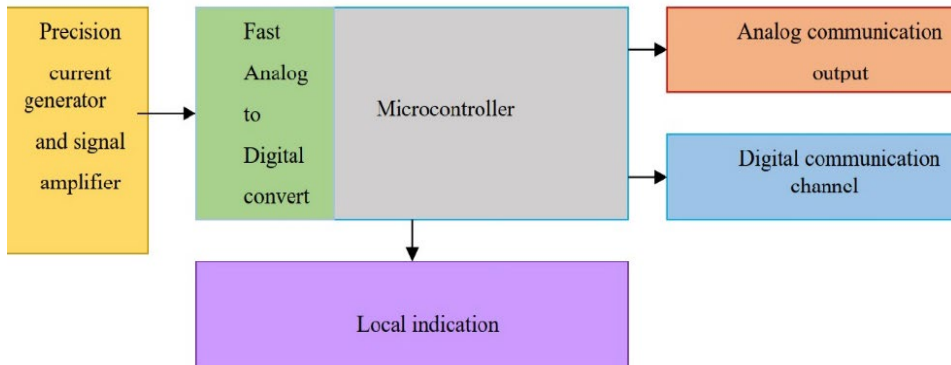


Fig. 3. Block Scheme of the developed communication concept of the therapeutic instrument

For the software implementation of the wireless microcontroller used in the design of the control system for the tool, the following can be noted that microcontroller function as network nodes of the designed specialized PLAN and use IEEE 802.15.4 resources [35]. All of them are programmed as network coordinators (in the sense of IEEE 802.15.4) of local autonomous networks that do not have end devices, i.e. each network contains only its coordinator (see Fig. 4).

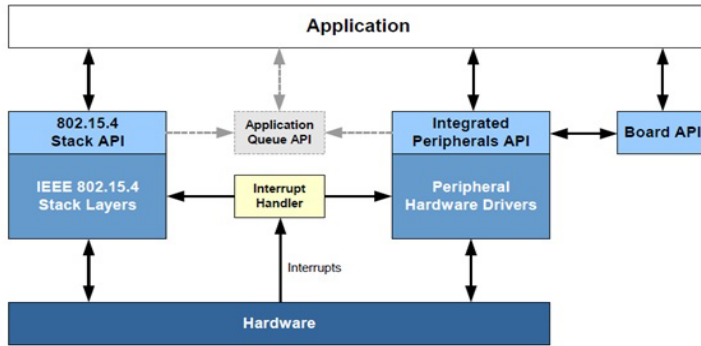


Fig. 4. Software architecture of IEEE 802.15.4

In the case where the user has to build his program using a large number of complex structures and functions of the various libraries, the application code becomes cumbersome and creates opportunities for errors that are difficult to debug. To solve this inconvenience is built Simple wireless network stack SWNS (Fig. 5).

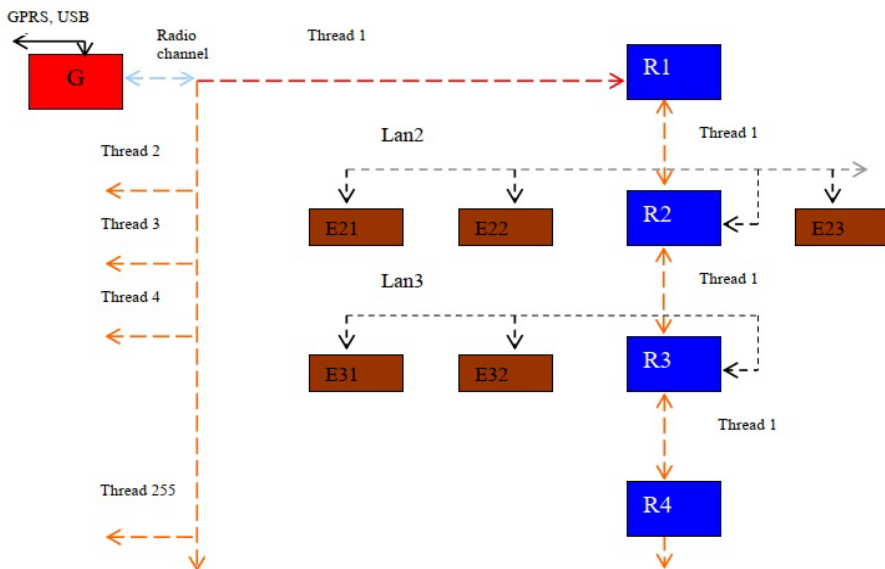


Fig. 5. Wireless network based on SWNS stack.

The notation in Fig. 5 are as follows: G –gateway device; R_i –router device (the device functions as router but is programmed as IEEE 802.15.4 coordinator); E_{ij} –end device j (it belongs to router R_i); Thread i -logical thread i ; Lan i – WLAN belongs to R_i ; Radio channel – radio channel, common for all wireless network devices.

The main features of SWNS are:

- SWNS is realized for wireless networks with nodes that being fully functional devices (FFD).
- SWNS is designed for three functional types of devices – gateway (G), routers (R) and end devices (E).
- All devices into wireless network have one predefined radio-channel.
- Each wireless network includes one device of type G , a number of devices of type R and a number of devices of type E .

Communication between microcontrollers is carried out as communication between networks using a predefined radio channel and “broad cast” messages. In order for them to work together, each of the networks must have a unique PAN identifier, which is defined and set as:

$$\text{PAN_ID} = \langle \text{device_number} \rangle + 256 * \langle \text{radiochannel_number} \rangle$$

A programmatic implementation has been discussed in detail in previous studies [36, 37] and the present work uses basic concepts with an upgrade. A similar concept is used in Projection System for Flexible Manufacturing [38].

In this particular case, the microcontroller functioning as the coordinator has $\langle \text{device_number} \rangle = 1$, the instrument controller – 2, and the radio channel being used $\langle \text{radiochannel_number} \rangle = 16$. The communication infrastructure and firmware in all microcontrollers of the wireless network controlling this instrument are the same.

3. Mode for studying the biomechanical properties of tissues

When performing laparoscopic operations with robotic systems, the hardware and software tools providing information on the contact points of the instrument with the tissue are important. This information must be received in a timely manner and synchronously with the management of the realized movements and be the basis for accepting various decisions from the control device, including the impact of local radiation sources with controllable intensity on tumor cells. A method of macro- and micro-stimulation was used to detect deviations in tissue parameters. It allows real-time monitoring of the “Relaxation Time” parameter, which determines the structure and mechanical properties of biological tissue. The macro and micro stimulation method includes a robot tool with incorporated force sensors. The force is measured by the sensors in the direction opposite to the instrument displacement. The instrument displacement is implemented through a sequence of single linear steps with identical length and direction, called macro stimuli. The tool-tissue interactions are implemented through an end-effector at the tool tip. Every macro stimulus leads to micro displacements (micro stimuli) at

the contact tissue point in a direction perpendicular to the contact tangential plane. The micro-stimuli interact with the tissue and lead to its reaction, which modulates the stress and forms a micro force in a direction opposite to the micro displacement. The total sum of micro forces (its component in the direction of the tool displacement) is counted by a tactile sensor. It is used in the assessment of the tissue structure. In the following text, the operation of a robotic tool with a conical shape of the end-effector will be investigated. The end effector is shaped conically with an angle of the tip 2α . The translation of the end-effector is a result of a single macro stimulus with equal steps L_0 and a direction defined by the straight line $O-OI$. After each step, the contact point of the tissue and the tool performs a micro displacement in a direction perpendicular to $O-OI$ with a length D_1 , which leads to a micro stimulus with a length L_1 (a micro displacement perpendicular to the tangent plane to the conical contact point). The tissue reaction is the generation of the micro force F_m . Its component in the direction of the displacement of the tool F_{mt} and the similar components of the micro forces generated at the other contact points are summed up and measured by the incorporated tactile sensor. A series of measurements is performed according to a pre-set time interval [39, 40, 41].

Fig. 6 shows the movement of the end-effector, which is done via a sequence of macro stimuli, each having a length L_0 in a predefined direction [42].

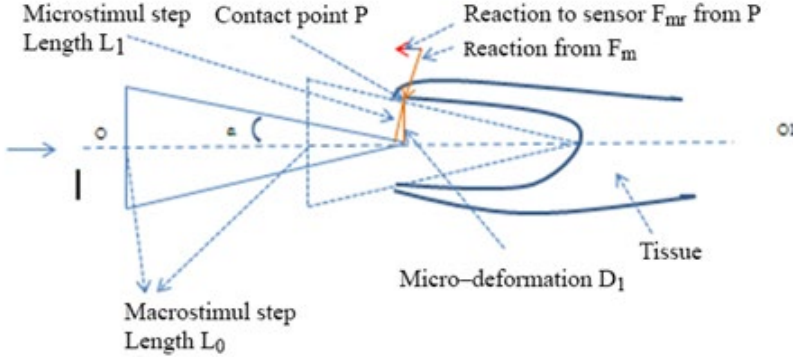


Fig. 6. End-effector movement.

Every macro stimulus generates micro stimuli and micro displacements with a length of L_1 at the contact points of the tissue. The following equation holds:

$$L_1 = L_0 \sin \alpha \quad (1)$$

The exceptions are the new contact points that occur when the tip of the tool interacts with the tissue. They are located on the surface on the cone, which

is bound by its tip and its cross-section with a plane perpendicular to the axis $O-OI$ and located at a distance L_0 from its tip.

At these points, the micro displacements are determined by:

$$L_1 = r \quad (2)$$

where r ranges from 0 to L_0 .

From Maxwell model for viscous elastic tissues where:

$$\sigma(t) = \xi_0 \times E_{rel}(t) = \xi_0 \times E \times e^{-\frac{t}{\tau}} \quad (3)$$

It follows that:

$$\sigma(t) = \xi \times E \times e^{-\frac{t}{\tau}} \quad (4)$$

ξ is one monotonous function $P(L_1)$, whose value is constant during the test measurements of σ :

$$\xi = P(L_1) \quad (5)$$

It can be rewritten as:

$$\sigma(t) = P(L_1) \times E \times e^{-\frac{t}{\tau}} \quad (6)$$

The stress $\sigma(t)$ at the point q in a constant tissue area can be defined by the reaction of its deformation L_1 and it is a function of the time. If $\Delta S(q)$ is the area of a micro-surface within the end-effector surface, in which there is a contact point q with stress σ , then a micro-force is formed on this micro-surface, whose projection $F_{mt}(p)$ on the axis $O-OI$ can be defined as:

$$F_{mt}(p) = \sin \alpha \times \Delta S(q) \quad (7)$$

Summing up $F_{mt}(p)$ at all contact points q , it is received the force which is measured by the tactile sensor at a given moment:

$$F = \sum_{q \in \{\text{contact points}\}} (F_{mt}(q)) \equiv F_{mt}(p) \quad (8)$$

To refine the estimate of the magnitude of the force F , which is measured by the tactile sensor, let us examine in detail the force interaction between the tool and the tissue. The conical manipulator can be regarded as being composed of two segments:

1. **K0**, which includes the points of the conical surface that are at a distance or less than or equal to L_0 (the length of the macro-stimulation steps) from the plane, which is orthogonal to the axis $O-OI$ and passes through its tip. **K0** creates new contact points with the tissue and equation (2) is in force.

2. **K1** includes the points of the cone surface which are located at a distance larger than L_0 (the length of macro-stimulus steps) from the plane which is orthogonal to the axis $O-OI$ and passes through its tip. **K1** always interacts with contact points which have already been created and for which equation (1) is in force. In Fig. 7, the segmentation of the conical end-effector is shown.

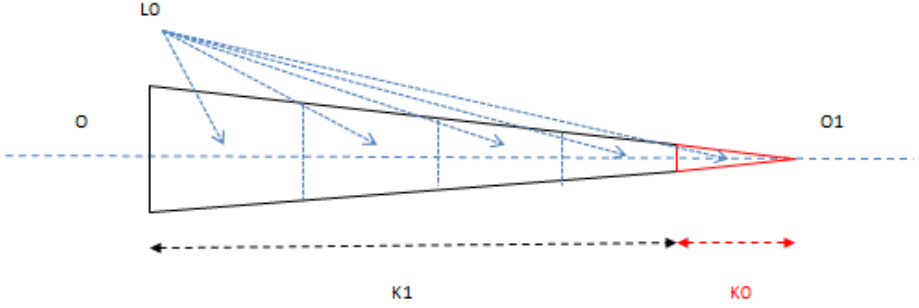


Fig. 7. Segmentation of the conical end-effector.

The tool performs a sequence of movements. Each one is the result of a macro-stimulus and generates translation movement with a step L_0 . As a result, the segments **K0** and **K1** perform a displacement of the contact points at a distance L_1 perpendicular to the surface of the cone and determined by equation (2) or equation (1), respectively. The tissue reacts at each contact point and a micro force F is formed along the axis $O-OI$ and the total force F is obtained by equation (8):

$$F = F_0 + F_1 \quad (9)$$

where F_0 is the sum of the force reactions formed at the contact points of the tissue with **K0** and F_1 is the sum of the force reactions formed at the contact points of the tissue with **K1**.

When performing a sequence of macro stimulations, the force measured by the sensors tends to increase. This is due to the increase in the number of contact points in a series of consecutive macro stimulations:

1. For the first macro stimulus this includes only the new contact points that are formed by **K0**;
2. For the second macro stimulus, this includes the new contact points that are formed by **K0** and the existing contact points that are formed by **K1**;
3. For the $n + 1$ stimulus, this includes the new contact points that are formed by **K0** and the existing contact points that are formed by **K1_n**;

The reaction of the tissue to every segment **K0**, **K1₁**, ..., **K1_n** is as follows generates a corresponding force that is measured by the sensor. In the general case, for predefined L_0 and α , the tissue reaction measured by the tactile sensor for the n^{th} macro stimulus can be written as:

$$F_n = F_0 + F_{1_n} \quad (10)$$

It can be shown that there is a common multiplier $e^{-\frac{t}{\tau}}$ in both addends on the right side of equation (10) because of which:

$$F_n = e^{-\frac{t}{\tau}} \times M(L_0, E, \alpha, n) \quad (11)$$

where: F_n is the force measured for the n^{th} macro stimulus.

The function $M(L_0, E, \alpha, n)$ depends on the parameters of the tool, the elastic modulus of the tissue E , and the sequential index n of the macro stimulus. A characteristic of this function is that it does not change its value during the time necessary to perform the macro stimulus. Due to this reason, the force F_n can be measured at the beginning of the second phase of the macro stimulus (for $t = 0$). Subsequently, the value of τ can be determined through a series of measurements.

Each macro stimulus includes two phases of implementation: generation of a translation step that performs a manipulator move. During the execution of this phase, a force is applied to the manipulator, which is sufficient to ensure that the displacement is carried out and to create a deformation of the examined tissue; retention phase starting after the successful completion of the first phase. During this phase, a holding force is formed on the manipulator, which is smaller than the displacement force, but guarantees the preservation of the translational movement performed during the first phase. During the second phase, a series of measurements of the force generated by the tissue response are performed sequentially over time. This is done through a tactile sensor built into the manipulator

Fig. 8 shows a timing diagram representing the execution of two macro stimulus, as well as the values of the control and measured quantities for the device providing their implementation.

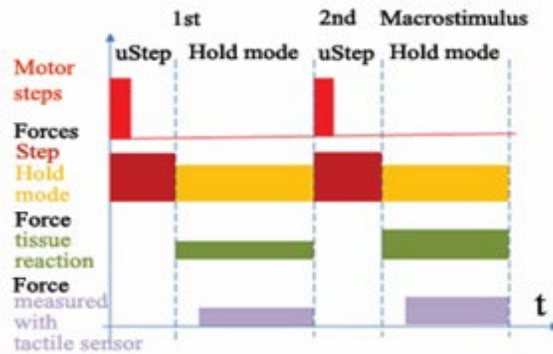


Fig. 8. A timing diagram representing the execution of two macro stimuli

The hold mode ensures the correct reading of the reaction force by the tactile sensor and the processing of this data by the micro controller. By generating macro stimulus with a step of small length, it is possible to precisely scan the change along the $O-OI$ axis of the manipulator and precisely locate the areas where there are sharp changes in the measurement values. The latter makes the method useful for real-time diagnostics, characterization of tissue biomechanical properties, and feedback in robotic instruments.

4. Therapeutics mode

After the first mode for studying the biomechanical properties of tissues is implemented, the device goes into therapy mode. An instrument is designed for programmable tissue exposure in the frequency range from 0 Hz to 500MHz or 40 MHz до 8 GHz. The irradiation is local. A programmed change in the intensity and frequency of the radio signal is a function of time. A basic idea is to transport the end of the tool where is embedded UFR emitter and therapy to be executed locally [43, 44].

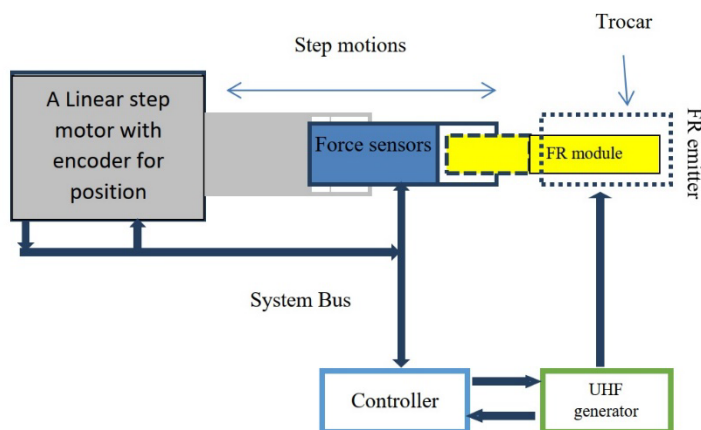


Fig. 9. An instrument for therapy with application in laparoscopy

The instrument uses an UHF Generator that generates a programmed frequency, forms the required radio signal through the output stage, and outputs it to an emitter to perform radiotherapy via a wired channel. The linear displacement of the module and its positioning at a set point is provided by the main step motor, taking into account force sensors readings to confirm the contact with the object of the therapy. The UHF Generator is external device, controlled by Controller and generates the signal to the UFR emitter.

External device generating a programmable frequency for Radiotherapy. The external device generating a programmable frequency for Radio Therapy is realized as a separate module (board), which is powered by 12VDC and forms,

through its emitting element, an electromagnetic field with a set programmed frequency and intensity in the patient's body. Generation control is mainly implemented by two integrated circuits - LMX2592 and AD9915. The former is controlled via SPI, using the SPI2 bus, while the latter uses the I2C bus. Both highways are supported by the ATxMega32A4, in its capacity as Master. The radiotherapy module is shown in Fig. 10.

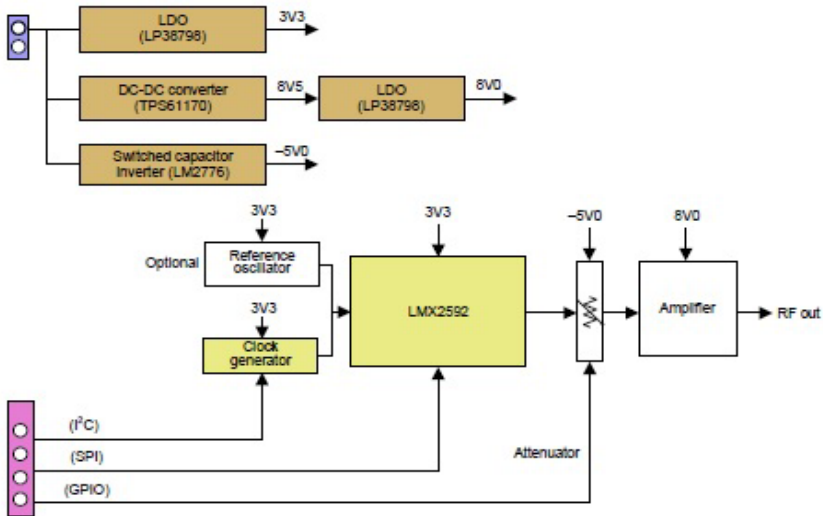


Fig. 10. Therapeutic module for a therapeutic device

The RF- generator is built on the base of programmable PLL generator LMX 2592, using programmable frequency reference source AD9915. Odd of them are being controlled by SPI and I2C from microcontroller ATxMega32A4, embedded in the main controller. The formed radio- signal is transmitted through wave- channel placed into the slider to the emitting block.

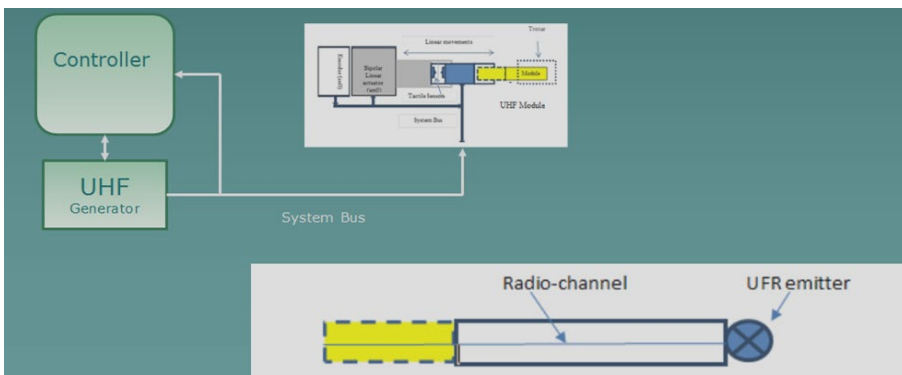


Fig. 11. RF therapy

Thus, through the SPI and I2C interfaces, the ATxMega32A4 manages the programmable generation of the output frequency of the electromagnetic field in the range of 0 to 8GHz. The external device can be controlled by any processor that has SPI and I2C interfaces. In our case, this processor is ATxMega32A4.4.

5. Experiments, Analyses and Results

In the first mode an Optimal control is defined as the optimization of certain predefined performance indices. Sometimes, parametric objective functions may be applied, for example, the linear quadratic optimal regulator problem where two weighting matrices need to be defined. Many optimal control problems can be converted in to conventional optimization problems by the powerful tools provided in MATLAB interface. Theoretical control solutions often neglected considerations on implementation of the controller.

In Table 1 are shown input and output experimental variables for necessary testing model. At this case the applied force is limited to 2 N. The experimental results are obtained with linear regression method by MATLAB interface which is shown on Fig. 12.

Table1. A table with input and output variables

Input / output variables [mm]	Experimental data				
	1	2	3	4	5
x	0	5	10	15	20
y	0	0.5	1	1.5	2

Linear regression model: $y = 0.1x - 3.4e - 016$

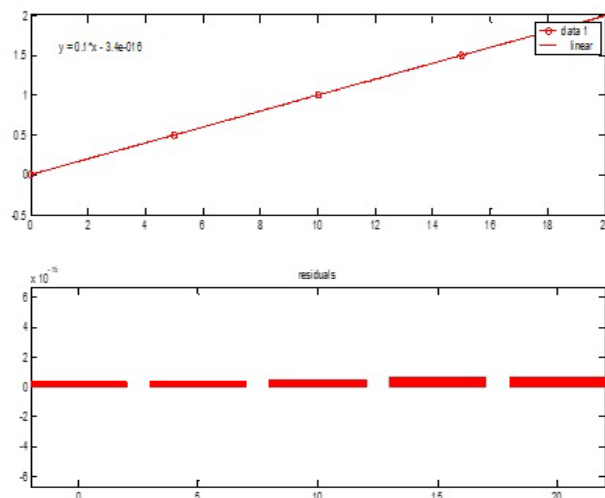


Fig. 12. Linear regression method for testing model

The experimental results are obtained with linear, quadratic and cubic regression method by MATLAB interface which is shown on Fig. 13.

In that (ideal) case Output date has to equal to input date (Output Force has to equal to input Force).

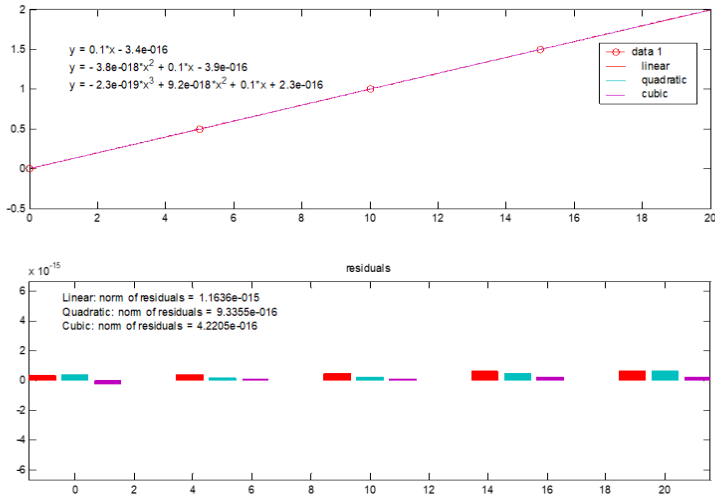


Fig. 13. Example for testing model by linear, quadratic and cubic methods. X = [0: 0.1500:15.0000] – input date; Y = [0:0.1500:15. 0000] – output date

The following example on the Fig. 14 is designed to illustrate the application of testing model of P-control for the family tools for laparoscopic surgery when no noise. Linear, quadratic and cubic methods are applied by MatLAB interface.

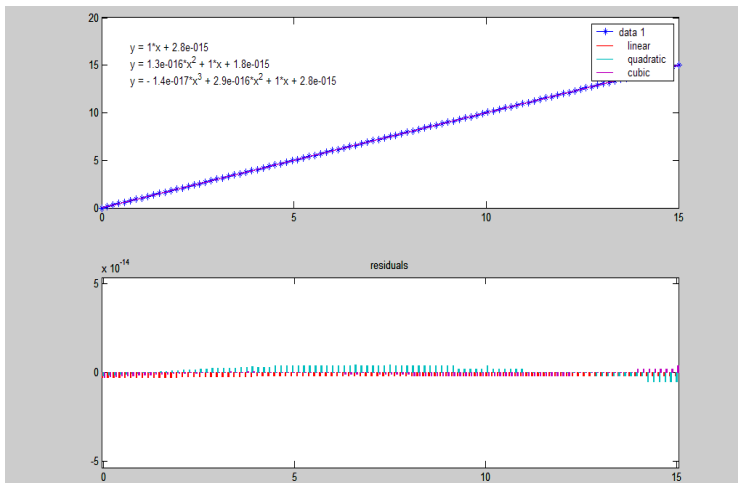


Fig. 14. Example for System with P Force control regulator.

Results obtained with the linear, quadratic and cubic methods for this input and output variables are approximately equals.

Experiments description: The program package that is used also includes a program for testing and set up the operation of the device. It allows testing and visualization of the results. Much of the capabilities of the software package have been described in detail in previous studies [45, 46] The purposes of carried out experiments are to verify the functionality and working capacity of the tools, to evaluate practically whether the error introduced by the proposed module during its normal operation is well within the required target, to demonstrate the operation of the tools

The experiment includes a search in the work area for a deviation with a set force value. It is shown in the red graphic. The blue graph shows the frequency of the generated RF signal used to irradiate the subject –see on Fig. 15.

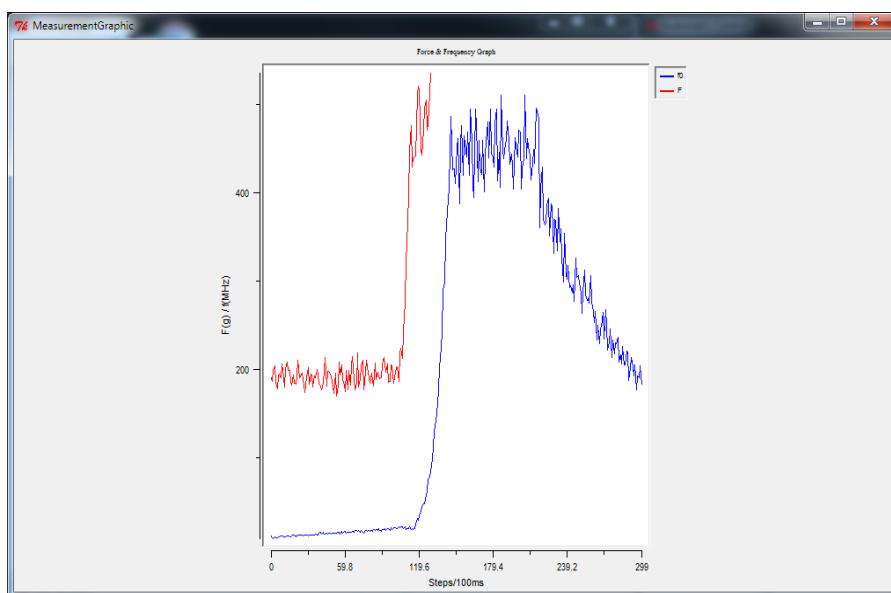


Fig. 15. Verify the functionality with Graphical presentation of the Experiments

When the deviation is detected, the formation of the micro steps is terminated and the generator starts operating in accordance with the set program. Upon reaching the set frequency, in the case of 434 MHz, radiation is maintained at the set frequency and intensity for the time defined by the therapy program - in this case 10 seconds. After that, the generator turns off and the frequency drops to the minimum.

The experimental results are presented in the Table 2.

Table 2. A table with experiment results.

	Fmin	Fmax	Amplitude
Search of a deviation – red graphic	200 F(g)/KMHz	450 F(g)/KMHz	250 F(g)/KMHz
Frequency of the generated RF signal – blue graphic	10 F(g)/KMHz	430 F(g)/KMHz	150 F(g)/KMHz

The number of the micro steps is located along the X-axis, along with the time in units of 100 ms. 100 ms is the time to take 1 micro step. Along the Y-axis is located the Force in grams, along X axis with the frequency of the irradiation signal in megahertz.

6. Conclusion and intentions for future work

In this article is describe our effort to design a therapeutic device to surgical robots for local tumor radiation. In contrast to other developments in the field of local tumor therapy, the paper discusses a device to surgical robots that simultaneously examines biomechanical tissue characteristics and applies local tumor therapy. The macro- and micro-stimulation method presented in this work is applied for diagnostic purposes and detects changes in the tissue structure. It allows the real-time monitoring of the relaxation time parameter, which gives information about the structure and mechanical properties of the biological tissue. After the first mode for studying of the biomechanical tissues properties is implemented, the device goes into therapy mode. A basic task of the therapy mode is to transport the end of the tool where is embedded UFR emitter and therapy to be executed locally at a given point with a set radiation.

The future work includes some experiments which have to be made with various frequency and intensity, and the results can be compared with different materials of similar properties of human tissues.

References

- 1 Lafon, C., Melodelima, D., Salomir, R., Chapelon, J.Y.: Interstitial devices for minimally invasive thermal ablation by high-intensity ultrasound. *International Journal of Hyperthermia* 23(2), 153–163, <https://doi.org/10.1080/02656730601173029> (2007)
- 2 Izadifar, Z., Izadifar, Z., Chapman, D., Babyn, P.: An introduction to high intensity focused ultrasound: Systematic review on principles, devices, and clinical applications. *Journal of Clinical Medicine* 9(2), 460, 1–22, DOI:10.3390/jcm9020460 (2020)

- 3 Cline, H.E., Hynynen, K., Watkins, R.D.; Adams, W.J., Schenck, J.F., Ettinger, R.H., Freund, W.R., Vetro, J.P., Jolesz, F.A.: Focused US system for MR imaging-guided tumor ablation. *Radiology* 194, 731–737 (1995)
- 4 Hynynen, K., Hynynen, K., Damianou, C., Darkazanli, A., Unger, E., Schenck, J.F.: The feasibility of using MRI to monitor and guide noninvasive ultrasound surgery. *Ultrasound in Medicine and Biology* 19(1), 91–92 (1993)
- 5 Hynynen, K., Darkazanli, A., Unger, E., Schenck, J.: MRI-guided noninvasive ultrasound surgery. *Medical Physics* 20, 107–115 (1993)
- 6 Yang, R., Reilly, C.R., Rescorla, F.J., Faught, P.R., Sanghvi, N.T., Fry, F.J., Franklin Jr, T.D., Lumeng, L., Grosfeld, J.L.: High-intensity focused ultrasound in the treatment of experimental liver cancer. *The Archives of Surgery* 126, 1002–1010, <https://doi.org/10.1001/archsurg.1991.01410320088012> (1991)
- 7 Goss, S.A., Fry, F.J.: The effect of high intensity ultrasonic irradiation on tumor growth. *IEEE Transactions on Sonics and Ultrasonics* 31, 491–496 (1984)
- 8 Zhou, Y.-F.: High intensity focused ultrasound in clinical tumor ablation. *World Journal of Clinical Oncology* 2(1), 8–27 (2011)
- 9 Dewey, W.C.: Arrhenius relationships from the molecule and cell to the clinic. *International Journal of Hyperthermia* 25(1), 3–20, (2009)
- 10 Haar, G.; Rivens, I.; Chen, L.; Riddler, S.: High intensity focused ultrasound for the treatment of rat tumours. *Physics in Medicine and Biology* 36(11), 1495–1501 (1991)
- 11 Klingler, H.C., Susani, M., Seip, R., Mauermann, J., Sanghvi, N., Marberger, M.J.: A novel approach to energy ablative therapy of small renal tumours: Laparoscopic high-intensity focused ultrasound. *European Urology* 53(4), 810–818 (2008)
- 12 Illing, R., Kennedy, J., Wu, F., Ter Haar, G., Protheroe, A., Friend, P., Gleeson, F., Cranston, D., Phillips, R., Middleton, M.: The safety and feasibility of extracorporeal high-intensity focused ultrasound (HIFU) for the treatment of liver and kidney tumours in a Western population. *British Journal of Cancer* 93, 890–895 (2005)
- 13 Köhrmann, K.U., Michel, M.S., Gaa, J., Marlinghaus, E., Alken, P.: High intensity focused ultrasound as noninvasive therapy for multilocal renal cell carcinoma: Case study and review of the literature. *Journal of Urology* 167, 2397–2403 (2002)
- 14 Wu, F., Wang, Z.-B., Chen, W.-Z., Bai, J., Zhu, H., Qiao, T.-Y.: Preliminary experience using high intensity focused ultrasound for the treatment of patients with advanced stage renal malignancy. *Journal of Urology* 170, 2237–2240 (2003)
- 15 Arya, M., Ahmed, H.U., Scardino, P., Emberton, M.: *Interventional Techniques in Uro-Oncology*. John Wiley & Sons: Hoboken, NJ, USA, p. 199 (2011)
- 16 Wu, F., Chen, W.Z., Bai, J., Zou, J.Z., Wang, Z.L., Zhu, H., Wang, Z.B.: Pathological changes in human malignant carcinoma treated with high-intensity

- focused ultrasound. *Ultrasound in Medicine and Biology* 27(8), 1099–1106 (2001)
- 17 Wu, F., Wang, Z.B., Chen, W.Z., Wang, W., Gui, Y., Zhang, M., Zheng, G., Zhou, Y., Xu, G., Li, M., et al.: Extracorporeal high intensity focused ultrasound ablation in the treatment of 1038 patients with solid carcinomas in China: An overview. *Ultrason. Sonochem*, 11, 149–154 (2004)
 - 18 Li, C.X., Xu, G.L., Jiang, Z.Y., Li, J.J., Luo, G.Y., Shan, H.B., Zhang, R., Li, Y.: Analysis of clinical effect of high-intensity focused ultrasound on liver cancer. *World Journal of Gastroenterol* 10, 2201–2204 (2004)
 - 19 Haar, G., Acoustic surgery. *Physics Today* 54, 29–34 (2001)
 - 20 Wu, F., Wang, Z.B., Chen, W.Z., Zou, J.Z., Bai, J., Zhu, H., Li, K.Q., Jin, C.B., Xie, F.L., Su, H.B.: Advanced hepatocellular carcinoma: Treatment with high-intensity focused ultrasound ablation combined with transcatheter arterial embolization. *Radiology* 235, 659–667 (2005)
 - 21 Huber, P.E., Jenne, J.W., Rastert, R., Simiantonakis, I., Sinn, H.-P., Strittmatter, H.-J., von Fournier, D., Wannemacher, M.F., Debus, J.: A new noninvasive approach in breast cancer therapy using magnetic resonance imaging-guided focused ultrasound surgery. *Cancer Research* 61, 8441–8447 (2001)
 - 22 Hynynen, K., Pomeroy, O., Smith, D.N., Huber, P.E., McDannold, N.J., Kettenbach, J., Baum, J., Singer, S., Jolesz, F.A.: MR imaging-guided focused ultrasound surgery of fibroadenomas in the breast: A feasibility study. *Radiology* 219, 176–185 (2001)
 - 23 Peek, M., Wu, F.: High-intensity focused ultrasound in the treatment of breast tumours, *Eancer Medical Science* 12, 794, <https://doi.org/10.3332/ecancer.2018.794>, (2018)
 - 24 Wu, F., Wang, Z.-B., Zhu, H., Chen, W.-Z., Zou, J.-Z., Bai, J., Li, K.-Q., Jin, C.-B., Xie, F.-L., Su, H.-B.: Extracorporeal high intensity focused ultrasound treatment for patients with breast cancer. *Breast Cancer Research and Treatment* 92, 51–60 (2005)
 - 25 Frizzell, L.A.: Threshold dosages for damage to mammalian liver by high intensity focused ultrasound. *IEEE Transactions on Ultrasonics, Ferroelectrics and Frequency Control* 35, 578–58 (1988)
 - 26 Gelet, A., Chapelon, J.Y., Bouvier, R., et al.: Transrectal high-intensity focused ultrasound: minimally invasive therapy of localized prostate cancer. *Journal of Endourology* 14, 519–528 (2000)
 - 27 Shi, X., Martin, R., Rouseff, D., Vaezy, S.: Detection of high intensity focused ultrasound liver lesions using dynamic elastometry. *Ultrason Imaging* 21(2), 107–126 (1999)
 - 28 Sibille, A., Prat, F., Chapelon, J.Y., et al.: Extracorporeal ablation of liver tissue by high intensity focused ultrasound. *Oncology* 50, 375–379 (1993)
 - 29 Gandini, A., Melodelima, D., Schenone, F., N'Djin, A. W., Chapelon, J. Y., Rivoire, M.: High-intensity focused ultrasound (HIFU)-assisted hepatic

- resection in an animal model. *Annals of Surgical Oncology* 19, 447–454 DOI: 10.1245/s10434-011-1875-0 (2012)
- 30 Konings, K., Vandevoorde, C., Baselet, B., Baatout, S., Moreels, M.: Combination therapy with charged particles and molecular targeting: A promising avenue to overcome radioresistance. *Frontiers in Oncology* 10(128), DOI: 10.3389/fonc.2020.00128 (2020)
 - 31 Sgurev, V.: Analysis of the contributions of Bulgarian Academy of Sciences in development and production of the industrial robots. *Problems of Engineering Cybernetics and Robotics* 73, 65–73, DOI: 10.7546/PECR.73.20.07 (2020)
 - 32 Wang, R.S., Ambani, S.N.: Robotic surgery training: Current trends and future directions. *Urologic Clinics of North America* 48(1), 137–146, <https://doi.org/10.1016/j.ucl.2020.09.014>, (2021)
 - 33 Maza, G., Sharma, A.: Past, present, and future of robotic surgery. *Otolaryngologic Clinics of North America* 53(6), 935–941 (2020)
 - 34 Borissova, D., Mustakerov, I.: Methodology for design of Web-based laparoscopy e-training system. *European Journal of Open, Distance an E-Learning*, 2, 1–9, ERIC Number: EJ954909, (2011), Available: <https://eric.ed.gov/?id=EJ954909>
 - 35 IEEE 802.15.4 Stack, User Guid., NXP Laboratories UK, (2015), Available from <https://www.nxp.com/docs/en/user-guide/JN-UG-3024.pdf>
 - 36 Bachvarov, D., Boneva, A., Boneva, Y., Angelov, S.: Simple wireless stack, based on IEEE 802.15.4, used for process – control applications. In: Proc. of International Conference on Big Data, Knowledge and Control Systems Engineering – BdKCSE'2016, John Atanasoff Society of Automatics and Informatics, pp. 71–79, (2016)
 - 37 Batchvarov, D., Boneva, A., Ilcheva, Z., Angelov, S., Ivanova, V.: Tools for control of mechatronic objects using the wireless network stack uMAC. In: Proc. of International Conference Automatics and Informatics'2017, 4-6 October 2017, 2. Session: Robotics and Mechatronics, John Atanasoff Society of Automatics and Informatics, Sofia, Bulgaria, pp. 77–80 (2017)
 - 38 Ilchev, S., Andreev, R., Ilcheva, Z., Otsetova-Dudin, E.: Computer-aided laser projection system for flexible manufacturing. In: Proc. of the 10th IEEE International Conference on Intelligent Systems (IS'20), Varna, Bulgaria, August 28-30, pp. 568–573, DOI: 10.1109/IS48319.2020.9199938 (2020)
 - 39 O'Zkaya, N., Nordin, M., Goldsheyder, D., Leger, D.: *Fundamentals of Biomechanics: Equilibrium, Motion, and Deformation*. Springer, DOI 10.1007/978-1-4614-1150-5 (2012)
 - 40 Dagnini, G.: *Laparoscopy and Imaging Techniques*. Springer, DOI:10.1007/978-3-642-74645-1 (2012)
 - 41 Knudson, D.: *Fundamentals of Biomechanics*. Springer, (2007)
 - 42 Ivanova, V., Batchvarov, D., Boneva, A.: A smart laparoscopic instrument with different application. *International Journal of Bioautomation* 24 (4), 403–417, DOI: 10.7546/ijba.2020.24.4.000723, (2019)

- 43 Ivanova, V., Batchvarov, D., Boneva, A., Ilcheva, Z.: A basic platform and electronics interfaces board for family therapeutics tools to surgical robots. *Global Journal of Researches in Engineering: H Robotics & Nano-Tech* 20(1), Version 1.0, 29–35, DOI: 10.17406/GJRE (2020)
- 44 Ivanova, V., Bachvarov, D., Boneva, A.: An Advanced Robot System for Diagnostic and Therapeutics Tasks with Application in Laparoscopic Surgery. *Journal of Computer Engineering & Information Technology* 7(2), 1–9, DOI: 10.4172/2324-9307.1000198 (2018)
- 45 Ivanova, V., Ilcheva, Z., Bachvarov D, Boneva, A.: Control system and software package for an experimental module with force feedback capabilities. In: *Proc. of Manufacturing Systems*, Romanian Academy Publishing House, 13(1), 3–10 (2018)
- 46 Ivanova, V.: Laparoscopic executive tools for robots. PhD Thesis, Institute of Robotics, Bulgarian Academy of Sciences, pp. 1-136, (2020), Available from http://ir.bas.bg/competitions/atanasova/avto_ata.pdf (in Bulgarian)